NANO LETTERS

Letter

pubs.acs.org/NanoLett

In Situ Investigation of Li and Na Ion Transport with Single Nanowire Electrochemical Devices

Xu Xu,[†,‡] Mengyu Yan,[†] Xiaocong Tian,[†] Chuchu Yang,[†] Mengzhu Shi,[†] Qiulong Wei,[†] Lin Xu,*[,§] and Liqiang Mai*[,†]

[†]State Key Laboratory of Advanced Technology for Materials Synthesis and Processing, Wuhan University of Technology, Wuhan 430070, China

[‡]Department of Chemistry and Biochemistry, University of California, Los Angeles, California 90095, United States

[§]Department of Chemistry and Chemical Biology, Harvard University, Cambridge, Massachusetts 02138, United States

Supporting Information

ABSTRACT: In the past decades, Li ion batteries are widely considered to be the most promising rechargeable batteries for the rapid development of mobile devices and electric vehicles. There arouses great interest in Na ion batteries, especially in the field of static grid storage due to their much lower production cost compared with Li ion batteries. However, the fundamental mechanism of Li and Na ion transport in nanoscale electrodes of batteries has been rarely experimentally explored. This insight can guide the development and optimization of high-performance electrode materials. In this work, single nanowire devices with multicontacts are designed to obtain detailed information during the electrochemical reactions. This unique platform is employed to in situ investigate and compare the transport properties of Li and Na ions at a single nanowire level. To give different confinement for ions and electrons during the electrochemical processes, two different configurations of nanowire electrode are proposed; one is to fully immerse the nanowire in the electrolyte, and the other is by using photoresist to cover the nanowire with only one end exposed. For both configurations, the conductivity of nanowire decreases after intercalation/deintercalation for both Li and Na ions, indicating that they share the similar electrochemical reaction mechanisms in layered electrodes. However, the conductivity degradation and structure destruction for Na ions is more severe than those of Li ions during the electrochemical processes, which mainly results from the much larger volume of Na ions and greater energy barrier encountered by the limited layered spaces. Moreover, the battery performances of coin cells are compared to further confirm this conclusion. The present work provides a unique platform for in situ electrochemical and electrical probing, which will push the fundamental and practical research of nanowire electrode materials for energy storage applications.

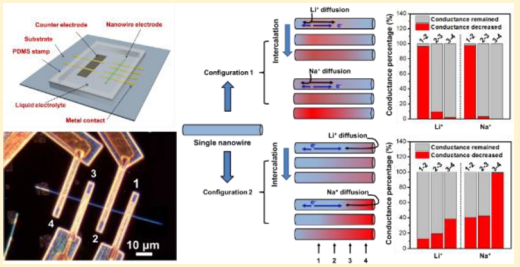

KEYWORDS: *Single nanowire electrodes, electrical transport, Na ion batteries, Li ion batteries*

High-performance energy storage devices are critical for the sustainable development of energy. Nowadays, Li-ion batteries are playing a more and more important role in the field of portable electronic devices and electronic vehicles.[1−3] Meanwhile, due to the low elemental abundance and the resulting high cost, researchers are trying to use Na ions as the charge carriers in electrochemical energy storage systems, which can be reversibly extracted from/inserted into layered materials like Li ions.[4,5] Some materials with the open crystal structure that allows Li ions intercalation also can be used in Na-ion batteries.[6] The comparison of Li and Na ion based energy storage systems have been reported, as they have the similar chemical properties in many aspects.[7−9] However, they mainly focus on the battery performance, such as the specific capacity, operation voltage, cyclability, and so forth. The fundamental mechanism of Li and Na ion transport in the nanoscale electrodes of batteries has been rarely experimentally explored.

Nanowires have the natural geometrical advantages for in situ electrochemical probing. With a length over tens of micrometers and diameter around tens of nanometers, a single nanowire electrode was built to in situ investigate the high-resolution structural and electrical evolution without the influence of nonactive materials during battery operation.[10,11] Huang et al. reported the first nanoscale electrochemical device inside a transmission electron microscope (TEM), which realized the in situ observation of the lithiation of the SnO_2 nanowire during electrochemical charging.[12] This advanced technique has been applied to other materials and electrochemical systems, including Na ion batteries.[13−15] However, this powerful tool still has several limitations. First, an ionic liquid or Li_2O (Na_2O in the case of Na ion batteries) are usually used in the high-vacuum TEM chamber, which makes

Received: February 20, 2015
Revised: April 29, 2015
Published: May 19, 2015

DOI: 10.1021/acs.nanolett.5b00705
Nano Lett. 2015, 15, 3879−3884

the electrochemical process different from real batteries with traditional liquid organic electrolytes. Second, the open-cell configuration design lacks diversity, and the nanowire electrode cannot be fully immersed in the liquid electrolyte like a real battery.[16,17] Importantly, in situ TEM can only provide the observation of morphology and structural changes, which are insufficient for electrochemical investigation. Our group has designed and assembled the smallest all-solid single nanowire electrochemical devices as a unique platform for in situ probing the direct correlation of electrical transport, structure, and electrochemistry.[18] Recently, a novel planar microbattery was designed to in situ measure the electrical transport during the charge and discharge of MoS_2 nanoflake electrode, which leads to the development of a novel charging strategy for batteries that largely improves the capacity and cycling performance confirmed in bulk MoS_2/Li coin cells.[19]

In this work, to further understand the transport characteristic of Li and Na ions in the nanoscale electrodes of batteries, multicontacts on single nanowire electrode are designed for recording the conductance of different parts of the nanowire at the charge/discharge status and giving detailed information. Furthermore, we introduce commercial liquid electrolytes instead of gel electrolytes in the devices to symbolize standard batteries and give insight for practical researches and applications.[18] With different electrolytes for lithium and sodium batteries, this unique platform is employed to in situ investigate and compare the migration properties of Li and Na ions at a single nanowire level, pushing forward the fundamental and practical research of nanowire electrode materials for energy storage applications.

Vanadium oxide nanowires with layered crystal structures have been reported as the host materials for both Li and Na ion intercalation.[5,20−25] Among them, $H_2V_3O_8$ nanowires would make the experimental results more accurate and reliable due to its high initial conductivity.[26] The single crystalline $H_2V_3O_8$ nanowires were synthesized by a hydrothermal method according to our previous work.[27,28] Figure S1 shows the structure and morphology characterization of the as-prepared nanowires. The nanowire grows along the [1 0 0] direction, with exposure of (0 0 8). The as-prepared $H_2V_3O_8$ nanowires are employed to fabricate the single nanowire electrochemical devices. As shown in the optical image and schematic (Figure 1), the device contains one $H_2V_3O_8$ nanowire as the cathode and one highly oriented pyrolytic graphite (HOPG) flake as the anode, and no other materials (such as binders or conductive additives) and introduced into the device.[29] The multipoint metal contacts are designed to realize the electrical transport tests of different parts of the single nanowire simultaneously, which can deeply reveal the electron and ion transport in the nanowire. In detail, three sections of the nanowire are divided by four metal contacts, and the electrical transport of each section is in situ tested separately. In order to fully investigate the ion transport in single nanowire, two different configurations of the nanowire electrode are adopted. For both configurations, metal contact 1 is used for electrochemical test, and the sections between contact 1 and 2, 2 and 3, and 3 and 4 are named section 1−2, 2−3, and 3−4, respectively.

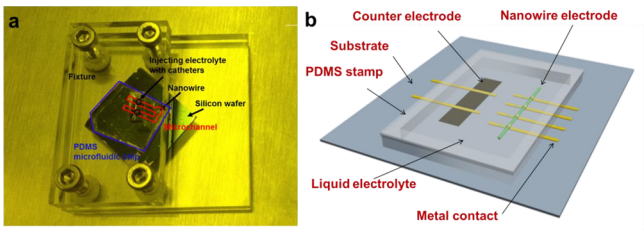

Figure 1. Structure of single nanowire electrode devices with multicontacts design and liquid organic electrolyte. (a) The optical image of the device. The device is sealed by a polydimethylsiloxane (PDMS) stamp with microchannels, in which the liquid electrolyte was injected to fully immerse the electrodes in an argon-filled glovebox, to ensure no exposing to air. (b) The overview of the device. Four metal contacts are integrated on one nanowire, and the liquid electrolyte is sealed into a PDMS stamp with microchannel.

The first configuration is that the nanowire is fully immersed into the electrolyte (Figure 2a), in which the Li or Na ions surround the entire nanowire. Figure 2b shows the dark field optical microscopic image of the nanowire electrode with the first configuration. The structure of $H_2V_3O_8$ nanowires is made up of V_3O_8 layers consisting of VO_6 octahedra and VO_5 distorted trigonal bipyramids interconnected with each other (Figure 2c). Thus, the Li or Na ions prefer transport through the *b*- or *c*-axis of the $H_2V_3O_8$ structure. *I*−*V* curves of three sections of the nanowire were recorded before and after the immersion of electrolyte (Figure S2). The uniform electrical conductivity and linear *I*−*V* curves indicate the high quality of nanowire structure as well as metal−nanowire contacts, and there was no conductance change after the immersion of electrolyte, indicating that the electrolyte would not destroy the structure without an electrochemical process. Meanwhile, the conductivity of the metal contact (Cr/Au) is over 1000 times higher than that of nanowire, which influences little on the transport characterization of nanowire. In this system, the conductivity (1709 S/m in average, including ion and electron transport) is much higher than ion transport (10^{-1}−10^{-3} S/m corresponding to the ion transfer coefficient of 10^{-12}−10^{-14} cm^2/s). Thus, the change of conductivity during electrochemical testing is mainly due to the degeneration of electron transport. Cyclic voltammetry (CV) was employed to drive the transport of electrons and ions between the cathode nanowire and anode.[30] With $LiPF_6$ as the electrolyte, CV curves with and without the nanowire at the scan rate of 0.5 mV/s are shown in Figure S3. Obvious peaks are observed with nanowire electrode, indicating the intercalation and deintercalation of the Li ions. Figure S4 shows the elemental analysis of HOPG flakes after the CV test. The solid electrolyte interphase is formed on the anode, which is the decomposition byproduct of electrolyte $LiPF_6$. As a control experiment, no F element on the flake is observed when it is immersed in electrolyte without reaction. This further proves that the electrochemical reaction take place on the nanowire cathode and HOPG anode.

As displayed in Figure 2a and b, contact 1 was used for both the electrochemical testing. The electrical transport of the three sections before and after the electrochemical processes were in situ recorded separately (Figure 2d−f for section 1−2, 2−3, and 3−4).[31] After the electrochemical reaction, the decreases of the nanowire conductance are 96.5%, 9.2%, and 1.9% for section 1−2, 2−3, and 3−4, respectively. The Li ion intercalation and deintercalation results in serious structural damage of the nanowire electrode, which is reflected by the sharp conductance decrease of section 1−2. However, for section 2−3, the decrease is only 9.2%, indicating that this part of the nanowire is only partly involved in the reaction. This phenomenon is more obvious for section 3−4, with a conductance decrease of 1.9%. It is worth noting that the nanowire is fully immersed in

DOI: 10.1021/acs.nanolett.5b00705
Nano Lett. 2015, 15, 3879−3884

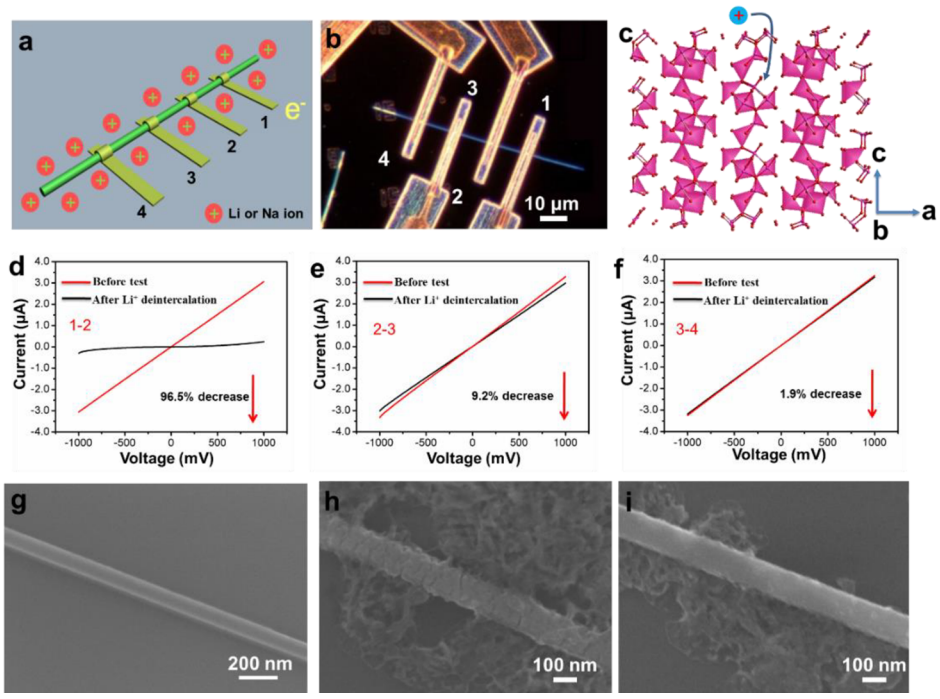

Figure 2. Single nanowire device with the first configuration. (a) The first configuration, in which the nanowire is fully immersed in the electrolyte. (b) The dark field optical microscopic image of the nanowire electrode. (c) The ion transport model for the first configuration. The V_3O_8 layer consisting of VO_6 octahedra and VO_5 distorted trigonal bipyramids interconnected with each other. The V atoms are pink, and O atoms are red. The ion can transport through *b* or *c* axis. (d–f) *I*–*V* curves of section 1–2, 2–3, and 3–4 before and after the electrochemical process, respectively. (g) SEM image of the $H_2V_3O_8$ nanowire before the reaction. (h, i) SEM images of section 1–2 and 2–3 after the reaction.

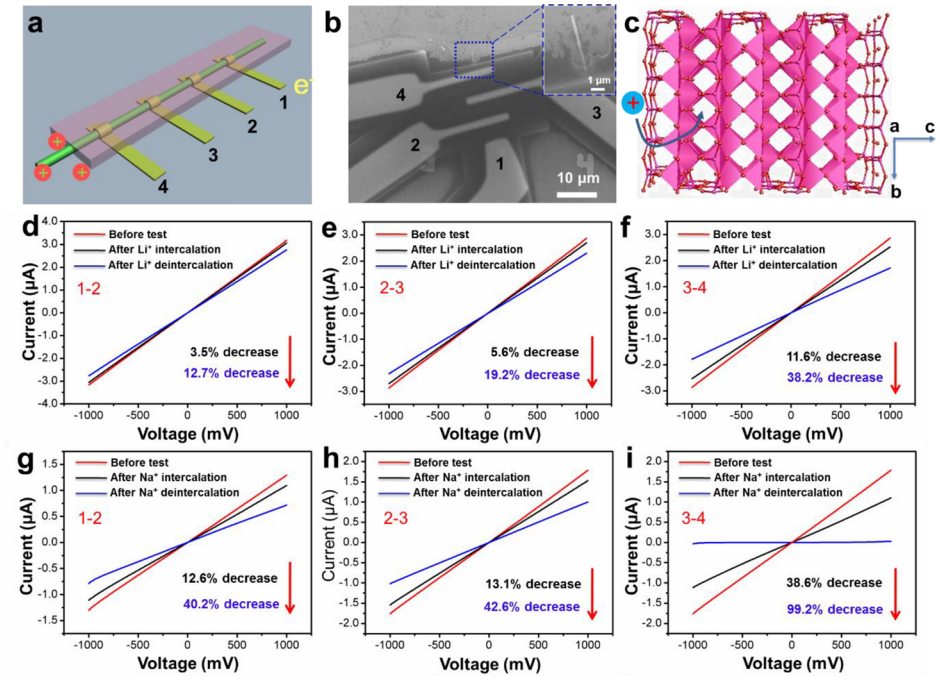

Figure 3. Single nanowire device with the second configuration. (a) The second configuration, in which the nanowire is covered by a passivation layer with only one exposed end. (b) The SEM image of the device with the second configuration. Only one end of the nanowire is exposed in the electrolyte (inset). (c) The ion transport model for the second configuration. The ions can only transport through the *a* axis of the $H_2V_3O_8$ nanowire. (d–f) *I*–*V* curves of section 1–2, 2–3, and 3–4 before and after the electrochemical processes for Li ions, respectively. (g–i) *I*–*V* curves of section 1–2, 2–3, and 3–4 before and after the electrochemical processes for Na ions, respectively.

the electrolyte in this configuration, in which the reaction region of nanowire mainly depends on the electron transport. The results indicate that the Li ions choose the shortest pathway along the radial direction to intercalate into the nanowire structure. The longer distance from the electron source makes the electron transport much more difficult, thus the section 2–3 and 3–4 are much less involved in the reaction. Moreover, the scanning electron microscopy (SEM) images

DOI: 10.1021/acs.nanolett.5b00705
Nano Lett. 2015, 15, 3879–3884

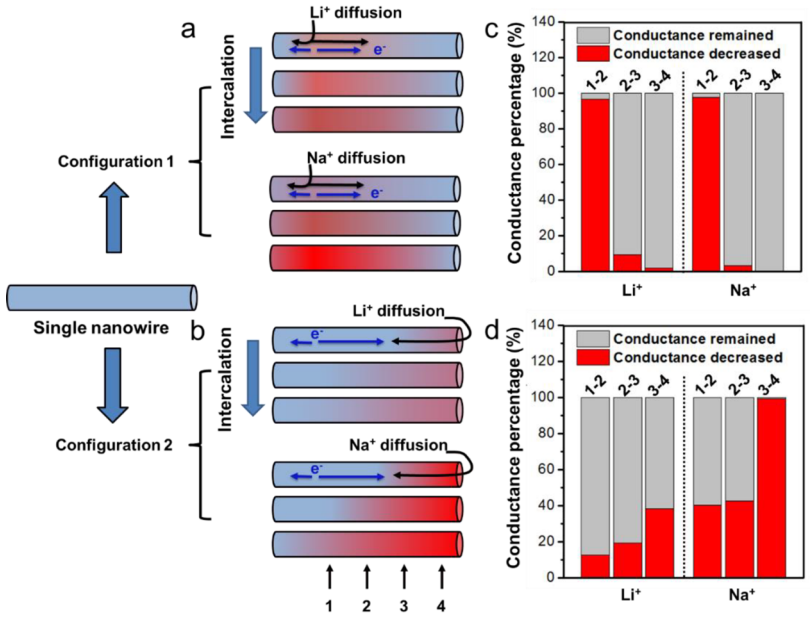

Figure 4. Schematic illustration and conductivity retentions of three sections after reation with Li and Na ions. (a, b) Schematic illustration of the Li and Na ions intercalation with two different device configurations. The red region of the nanowires represents the structure and conductivity degradation during intercalation. (c) The conductivity retentions of sections 1−2, 2−3, and 3−4 after intercalation/deintercalation with Li and Na ions for configuration 1, respectively. (d) The conductivity retentions of sections 1−2, 2−3, and 3−4 after intercalation/deintercalation with Li and Na ions for configuration 2, respectively.

after the reaction were collected to provide further evidence. Before the reaction, the nanowires have smooth surface without any other impurities (Figure 2g). After the intercalation and deintercalation of Li ions, The LiF is observed at both section 1−2 and section 2−3 of the nanowire. Section 1−2 of the nanowire cracks because of the deep intercalation and deintercalation of Li ions, while section 2−3 still maintains its initial smooth surface (Figure 2h,i). This result further proves that the electrochemical process mainly occurred in section 1−2 where the nanowire is severely damaged. In our previous report, the Raman mapping of single nanowire electrode was employed to in situ observe the structural change during the electrochemical reaction, which also confirms that the conductance decrease is caused by the structural degradation.[18] The device with the first configuration for Na ions gives a similar result as Li ions (Figure S5), manifesting that they have similar transport behavior in the layered structure of vanadium oxide.

The ultimate goal of the single nanowire electrochemical device research is to provide guidance to electrode design and modification for better batteries. For instance, the configuration discussed above may give some insight for the nanowire array electrode design, such as the silicon nanowire array on a conductive substrate,[32] in which the electrons can only transport into the nanowires from the end attached to the substrate, while the Li ions are available for the entire nanowire surface. From this single nanowire device study, researchers should consider the suitable length of the nanowire arrays, as the part further away from the attached end is harder to involve in the electrochemical reaction if the nanowire is too long. Furthermore, high conductivity of the nanowire may also have a positive effect to take full advantage of the nanowire electrode.

In order to further compare the transport properties of Li and Na ions, the second configuration is designed to confine the pathway of ions and electrons, in which the nanowire is covered by a passivation layer with only one end immersed in the electrolyte (typical SEM image in Figure 3b and optical image in Figure S6). The ions can only intercalate into the covered part of nanowire from the exposed end along the *a* axis direction (Figure 3a,c). With the purpose of getting detailed information, *I*−*V* curves of three sections were recorded separately at the initial stage, after the ions intercalation, and after the ions deintercalation, respectively. Same as configuration 1, contact 1 is also used for the CV test. At the initial stage, all the sections of the nanowire show uniform and high conductivity. After Li ions intercalation, the conductivity decreases of section 1−2, 2−3, and 3−4 are 3.5%, 5.6%, and 11.6%, respectively (Figure 3d−f). The values after Li ions deintercalation are 12.7%, 19.2%, and 38.2%, respectively. Noticeably, the further the distance from the electrochemical contact point is, the more the conductance decreases, corresponding to the more severe structural degradation of the nanowire. As predicted, the result of this configuration is totally different from the first one. For any part of the nanowire, the electrochemical process could only react when the electrons and ion are both available. Under this condition, Li ions and electrons can only proceed into the nanowire from opposite ends. This combination forces them to transport along the axial direction. Electrons have a much higher migration rate in the nanowire, so the reaction region is mainly limited by the Li ions due to their relatively low mobility. The conductance of the nanowire did not show dramatic and reversible change after the Li ions intercalate and deintercalate as our previous work,[18] which may result from the different electrode/electrolyte interface properties in liquid organic electrolyte and the different electrochemical driving forces. Similar phenomena are found when the charge carriers are Na ions, thus giving a clue that both ions share the similar electrochemical reaction mechanism in layered electrodes. The conductivity decreases after the Na ions intercalate in section 1−2, 2−3, and 3−4 are 12.6%, 13.1%, and 38.5%, respectively (Figure 3g−i). The

DOI: 10.1021/acs.nanolett.5b00705
Nano Lett. 2015, 15, 3879−3884

values after the Na ions deintercalate are 40.2%, 42.6%, and 99.2%, respectively.

The schematic illustration and conductivity retentions of section 1−2, 2−3, and 3−4 after reacting with Li and Na ions are further compared. As demonstrated above, the ions mainly inserted into the nanowire around contact 1 for the first configuration (Figure 4a). For the configuration 2, the ions can only move into the nanowire from opposite ends, which lead to the degeneration of conductivity (Figure 4b). Noticeably, the conductance decrease when Na ions intercalate is more severe than that of Li ions in the second configuration (Figure 4d). This indicates that the destruction degree of Na ions is more severe than that of Li ions during the electrochemical processes. As for the layered structure of $H_2V_3O_8$ nanowire, Li or Na ions mainly transport through the spaces between the stacked layers along the *a* axis, with a *d* spacing of 8.46 Å (see the crystal structure in Figure S7). For this certain size, it is more difficult for Na ions to transport, as a Na ion is 372% larger in volume than Li ion (R_{Li} = 59 pm, R_{Na} = 99 pm).[33] When the Na ions are electrochemically driven into the layers, they would encounter greater energy barrier , and the crystal structure is destroyed after the intercalation and deintercalation processes. This is not favorable for the cycling performance of rechargeable batteries. Interestingly, the phenomenon observed in configuration 1 is different from that in configuration 2. The conductivity decrease when Li ions intercalate is larger than that of Na ions in sections 2−3 and 3−4 (Figure 4c). That is due to the fact that the diffusion of Li ions is much faster than that of Na ions during the electrochemical processes. It is really hard for Na ions to diffuse to other sections from section 1−2 with such a confinement, as in configuration 2. To further confirm the point mentioned above, conventional coin batteries were assembled using $H_2V_3O_8$ nanowires as cathode active materials, for both Li and Na ions as charge carriers.[34] The initial specific discharge capacities of lithium and sodium batteries are 180 and 64 mAh/g, respectively (Figure S8). Meanwhile, the capacitance retention of sodium battery is only 70% after 60 cycles with the relative low Coulombic efficiencies around 92%, both of which are much lower than those of lithium battery (the capacity retention of 90% after 60 cycles and Coulombic efficiencies around 99%). The lower capacity and poorer cycling performance of vanadium oxide nanowires as a sodium battery cathode is consistent with the single nanowire devices study. With larger volume, sodium ions will encounter a higher ionization potential than Li ions intercalating into the same layered structure of vanadium oxide.[36,37] The intercalation and deintercalation of Na ions into the limited interlayer space leads to the crystalline structure change, which is accompanied by the electronic conductivity decrease and capacity loss.[5,18]

In summary, single nanowire electrochemical devices with organic liquid electrolyte are designed to investigate the Li and Na ion transport behavior, respectively. Two different configurations, one with the nanowire fully immersed in the electrolyte and the other with only a fraction of nanowire left exposed in electrolyte, are proposed to give different confinement for ions and electrons during the electrochemical processes. When the nanowire is fully immersed in the electrolyte, it is found that the ions would choose the shortest pathway along the radial direction to intercalate into the nanowire structure. For the second configuration in which the nanowire is covered by a passivation layer with only one exposed end, ions and electrons transport into the nanowire from opposite ends along the axial direction, where the reaction region is mainly limited by the ions due to their relatively low mobility than electrons. For both configurations, similar phenomena are observed when the charge carriers are Li and Na ions, indicating that they share similar electrochemical reaction mechanisms in layered electrodes. However, the crystal structure degradation by Na ions is more severe than that of Li ions during the electrochemical processes, which mainly results from the much larger volume of Na ions and the greater energy barrier encountered by the limited interlayer space. Single nanowire electrochemical devices will act as a unique platform to push the fundamental and practical research of nanowire electrode materials for energy storage applications.

■ ASSOCIATED CONTENT

Supporting Information

Additional information and figures. The Supporting Information is available free of charge on the ACS Publications website at DOI: 10.1021/acs.nanolett.5b00705.

■ AUTHOR INFORMATION

Corresponding Authors

*E-mail: mlq518@whut.edu.cn.

*E-mail: lxu@cmliris.harvard.edu.

Author Contributions

X. Xu and M. Y. Yan contributed equally to this work. L. Q. Mai, L. Xu, X. Xu, and M. Y. Yan designed the experiments. X. Xu, M. Y. Yan, X. C. Tian, and C. C. Yang performed the experiments. X. Xu, M. Y. Yan, X. C. Tian, and Q. L. Wei discussed the interpretation of results and cowrote the paper. All authors discussed the results and commented on the manuscript.

Notes

The authors declare no competing financial interest.

■ ACKNOWLEDGMENTS

This work was supported by the National Basic Research Program of China (2013CB934103, 2012CB933003), the National Natural Science Foundation of China (51302203, 51272197), the International Science & Technology Cooperation Program of China (2013DFA50840), The National Natural Science Fund for Distinguished Young Scholars (51425204), The Hubei Science Fund for Distinguished Young Scholars (2014CFA035), and the Fundamental Research Funds for the Central Universities (2013-ZD-7, 2014-YB-01, 2014-YB-02, 2014-VII-007). Thanks Professor Q. J. Zhang of Wuhan University of Technology for strong support and stimulating discussions. Special thanks are given to J. Liu of Pacific Northwest National Laboratory for his careful supervision, strong support, and stimulating discussions.

■ REFERENCES

(1) Kang, B.; Ceder, G. *Nature* **2009**, *458*, 190−193.

(2) Tarascon, J.-M.; Armand, M. *Nature* **2001**, *414*, 359−367.

(3) Kang, K.; Meng, Y. S.; Breger, J.; Grey, C. P.; Ceder, G. *Science* **2006**, *311*, 977−980.

(4) Yabuuchi, N.; Kajiyama, M.; Iwatate, J.; Nishikawa, H.; Hitomi, S.; Okuyama, R.; Usui, R.; Yamada, Y.; Komaba, S. *Nat. Mater.* **2012**, *11*, 512−517.

(5) Tepavcevic, S.; Xiong, H.; Stamenkovic, V. R.; Zuo, X.; Balasubramanian, M.; Prakapenka, V. B.; Johnson, C. S.; Rajh, T. *ACS Nano* **2011**, *6*, 530−538.

DOI: 10.1021/acs.nanolett.5b00705
Nano Lett. 2015, 15, 3879−3884

(6) Kim, S. W.; Seo, D. H.; Ma, X.; Ceder, G.; Kang, K. *Adv. Energy Mater.* **2012**, *2*, 710−721.
(7) Ong, S. P.; Chevrier, V. L.; Hautier, G.; Jain, A.; Moore, C.; Kim, S.; Ma, X.; Ceder, G. *Energy Environ. Sci.* **2011**, *4*, 3680−3688.
(8) Darwiche, A.; Marino, C.; Sougrati, M. T.; Fraisse, B.; Stievano, L.; Monconduit, L. *J. Am. Chem. Soc.* **2012**, *134*, 20805−20811.
(9) Luo, C.; Xu, Y.; Zhu, Y.; Liu, Y.; Zheng, S.; Liu, Y.; Langrock, A.; Wang, C. *ACS Nano* **2013**, *7*, 8003−8010.
(10) Lieber, C. M. *MRS Bull.* **2011**, *36*, 1052−1063.
(11) Tian, B.; Zheng, X.; Kempa, T. J.; Fang, Y.; Yu, N.; Yu, G.; Huang, J.; Lieber, C. M. *Nature* **2007**, *449*, 885−889.
(12) Huang, J. Y.; Zhong, L.; Wang, C. M.; Sullivan, J. P.; Xu, W.; Zhang, L. Q.; Mao, S. X.; Hudak, N. S.; Liu, X. H.; Subramanian, A. *Science* **2010**, *330*, 1515−1520.
(13) Liu, X. H.; Zhang, L. Q.; Zhong, L.; Liu, Y.; Zheng, H.; Wang, J. W.; Cho, J.-H.; Dayeh, S. A.; Picraux, S. T.; Sullivan, J. P. *Nano Lett.* **2011**, *11*, 2251−2258.
(14) Liu, X. H.; Huang, J. Y. *Energy Environ. Sci.* **2011**, *4*, 3844−3860.
(15) Gu, M.; Kushima, A.; Shao, Y.; Zhang, J.-G.; Liu, J.; Browning, N. D.; Li, J.; Wang, C. *Nano Lett.* **2013**, *13*, 5203−5211.
(16) Gu, M.; Parent, L. R.; Mehdi, B. L.; Unocic, R. R.; McDowell, M. T.; Sacci, R. L.; Xu, W.; Connell, J. G.; Xu, P.; Abellan, P. *Nano Lett.* **2013**, *13*, 6106−6112.
(17) Abellan, P.; Mehdi, B. L.; Parent, L. R.; Gu, M.; Park, C.; Xu, W.; Zhang, Y.; Arslan, I.; Zhang, J.-G.; Wang, C.-M. *Nano Lett.* **2014**, *14*, 1293−1299.
(18) Mai, L.; Dong, Y.; Xu, L.; Han, C. *Nano Lett.* **2010**, *10*, 4273−4278.
(19) Wan, J.; Bao, W.; Liu, Y.; Dai, J.; Shen, F.; Zhou, L.; Cai, X.; Daniel, U.; Li, Y.; Katherine, J.; Michael, S. F.; Hu, L. *Adv. Energy Mater.* **2015**, *5*, 1401742.
(20) Mai, L.; Xu, L.; Han, C.; Xu, X.; Luo, Y.; Zhao, S.; Zhao, Y. *Nano Lett.* **2010**, *10*, 4750−4755.
(21) Mai, L.; Xu, X.; Xu, L.; Han, C.; Luo, Y. *J. Mater. Res.* **2011**, *26*, 2175−2185.
(22) Xu, X.; Luo, Y.-Z.; Mai, L.-Q.; Zhao, Y.-L.; An, Q.-Y.; Xu, L.; Hu, F.; Zhang, L.; Zhang, Q.-J. *NPG Asia Mater.* **2012**, *4*, e20.
(23) Yan, M.; Wang, F.; Han, C.; Ma, X.; Xu, X.; An, Q.; Xu, L.; Niu, C.; Zhao, Y.; Tian, X. *J. Am. Chem. Soc.* **2013**, *135*, 18176−18182.
(24) Mai, L.; Dong, F.; Xu, X.; Luo, Y.; An, Q.; Zhao, Y.; Pan, J.; Yang, J. *Nano Lett.* **2013**, *13*, 740−745.
(25) Su, D.; Wang, G. *ACS Nano* **2013**, *7*, 11218−11226.
(26) An, Q.; Sheng, J.; Xu, X.; Wei, Q.; Zhu, Y.; Han, C.; Niu, C.; Mai, L. *New J. Chem.* **2014**, *38*, 2075−2080.
(27) Mai, L.; Wei, Q.; An, Q.; Tian, X.; Zhao, Y.; Xu, X.; Xu, L.; Chang, L.; Zhang, Q. *Adv. Mater.* **2013**, *25*, 2969−2973.
(28) The single crystalline $H_2V_3O_8$ nanowires were synthesized by a hydrothermal method according to our previous work. 100 μL of poly(ethylene glycol) (PEG 400) and 30 mL of V_2O_5 solutions were added into the distilled water to reach the total volume of 60 mL. The precursor was stirred for one day and aged for another one day, then transferred to a 100 mL Teflon lined autoclave and kept in an oven at 180 °C for 48 h. The product was washed and dried to get $H_2V_3O_8$ nanowires. The absence of aniline in the synthesis process would be helpful for the monodispersion of the nanowires.
(29) The anode HOPG flakes were first dry-transferred onto a marked substrate, and cathode vanadium oxide nanowires were then deposited onto the region close to the HOPG flakes. Multipoints metal contacts on single nanowire were patterned with e-beam lithography and deposition of Cr/Au (10/150 nm). A patterned SU-8 (SU8 2000.5, Micro Chem) resist layer was then fabricated over the metal contacts as passivation layer. The device area was then sealed with PDMS stamp with microchannels, and the liquid electrolyte (1 M $LiPF_6$ for Li-ion batteries or $NaClO_4$ for Na-ion batteries in a mixture of ethylene carbonate (EC)/dimethyl carbonate (DMC)) was then injected into through the microfluidic technology in an argon-filled glovebox.
(30) Cyclic voltammetry (CV) was carried out with an electrochemical workstation (Autolab PGSTAT 302N), with the devices electrically connected in the probe station (Lakeshore TTP4).
(31) The in situ *I*−*V* tests before and after the electrochemical processes were carried out with a semiconductor device analyzer (Agilent B1500A), with the devices electrically connected in the probe station.
(32) Chan, C. K.; Peng, H.; Liu, G.; McIlwrath, K.; Zhang, X. F.; Huggins, R. A.; Cui, Y. *Nat. Nanotechnol.* **2007**, *3*, 31−35.
(33) Dean, J. A. *Lange's Handbook of Chemistry*; McGraw-Hill, Inc.: New York, 1999; Vol. *4*.
(34) The 2025 coin cells were assembled in a glovebox. Cathode electrodes were obtained with 70% active materials, 20% acetylene black, and 10% poly(tetrafluoroethylene) (PTFE). For lithium batteries, lithium pellets were used as the anodes and 1 M $LiPF_6$ in EC/ DMC as electrolyte. For sodium batteries, sodium pellets and 1 M $NaClO_4$ in EC/DMC were used as the anodes and electrolyte, respectively. Galvanostatic charge/discharge cycling was studied in a potential range of 3.75−1.5 V with a multichannel battery testing system (LAND CT2001A).
(35) Raju, V.; Rains, J.; Gates, C.; Luo, W.; Wang, X.; Stickle, W. F.; Stucky, G. D.; Ji, X. *Nano Lett.* **2014**, *14*, 4119−4124.
(36) Kim, D.; Kang, S. H.; Slater, M.; Rood, S.; Vaughey, J. T.; Karan, N.; Balasubramanian, M.; Johnson, C. S. *Adv. Energy Mater.* **2011**, *1*, 333−336.
(37) Cao, Y.; Xiao, L.; Sushko, M. L.; Wang, W.; Schwenzer, B.; Xiao, J.; Nie, Z.; Saraf, L. V.; Yang, Z.; Liu, J. *Nano Lett.* **2012**, *12*, 3783−3787.

DOI: 10.1021/acs.nanolett.5b00705
Nano Lett. 2015, 15, 3879−3884